Enhancing the fracture toughness of carbon fibre/epoxy composites by interleaving hybrid meltable/non-meltable thermoplastic veils

Quan, Dong; Alderliesten, René; Dransfeld, Clemens; Murphy, Neal; Ivanković, Alojz; Benedictus, Rinze

DOI
10.1016/j.compstruct.2020.112699

Publication date
2020

Document Version
Final published version

Published in
Composite Structures

Composite Structures 252 (2020) 112699

Contents lists available at ScienceDirect

Composite Structures

journal homepage: www.elsevier.com/locate/compstruct

Enhancing the fracture toughness of carbon fibre/epoxy composites by interleaving hybrid meltable/non-meltable thermoplastic veils

Dong Quan [a,*], René Alderliesten [a], Clemens Dransfeld [a], Neal Murphy [b], Alojz Ivanković [b], Rinze Benedictus [a]

[a] Department of Aerospace Structures and Materials, Delft University of Technology, Netherlands
[b] School of Mechanical and Materials Engineering, University College Dublin, Ireland

ARTICLE INFO

Keywords:
Carbon fibre/epoxy composites
Thermoplastic veils
Hybrid toughening
Fracture toughness.

ABSTRACT

Interlaying thermoplastic veils into carbon fibre/epoxy composites has proved to significantly increase the interlaminar fracture toughness. The main toughening mechanism is thermoplastic fibre bridging for the non-meltable veils and matrix toughening for the meltable veils. Herein, to take advantage of different toughening mechanisms, hybrid meltable/non-meltable thermoplastic veils were used to interlay two types of aerospace-grade composites produced from unidirectional (UD) prepregs and resin transfer moulding of non-crimp carbon fibre fabrics (NCF). The mode-I and mode-II fracture behaviour of the interleaved laminates were investigated. The experimental results demonstrated outstanding toughening performance of the hybrid veils for the mode-I fracture behaviour of the UD laminates and for both of the mode-I and mode-II fracture behaviour of the NCF laminates, resulting from the combination of different toughening mechanisms. For example, the maximum increases in the mode-I and mode-II fracture energies of the NCF laminates were observed to be 273% and 206%, respectively.

1. Introduction

Carbon fibre reinforced epoxy (CF/EP) composites are prone to interlaminar delamination due to the inherent brittleness of epoxy matrix. Interleaving, i.e. inserting a discrete interlayer between adjacent plies is one of the most popular strategies to enhance the interlaminar fracture toughness of CF/EP laminates. Many types of interleaving materials have been used to reinforce CF/EP laminates, including carbon nanomaterials [1–4], thermoplastics [5–8] and other materials [9,10]. As the most prevalent interlayer materials of CF/EP laminates, thermoplastics in a shape of powder, film, scrim and non-woven fabric were all used for interlayer toughening [7,8,11]. Moreover, after the laminate curing, thermoplastic phases can exist in the laminates in different forms, such as being intact [12,13], molten during the laminate curing process [14,8] and partially or completely dissolved in the epoxy matrix [7,15]. For these reasons, the use of thermoplastic materials as interlayers allows researchers to tailor the mechanical and fracture properties of CF/EP laminates by adjusting the content, shape and form of the thermoplastic materials in them.

Interlaying non-woven thermoplastic veils based on micro-/nanoscale fibres has proved to significantly enhance the interlaminar fracture toughness of CF/EP laminates, e.g. above 200% increases in the fracture energies were obtained in [14,16–19]. Additionally, no decreases in the stiffness [12,15,20,21] and strength [12,19,20,22] of the laminates were observed upon interleaving thermoplastic veils. In our previous studies [14,16], the toughening efficiency of thermoplastic veils for aerospace-grade CF/EP laminates has been systematically investigated. Thermoplastic veils consisting of micro-scale Polyethylene terephthalate (PET), Polyphenylene sulfide (PPS) and Polyamide-12 (PA) fibres were used as interlayer materials of three types of aerospace-grade CF/EP laminates manufactured by unidirectional (UD) prepegs, 5-Harness satin weave (5H) prepregs and resin transfer moulding (RTM) of non-crimp carbon fibre fabrics (NCF). All the laminates were cured at 180 °C for 2 h, during which, the PET and PPS veils remained intact and the PA veils melted. While significant improvements in both of the mode-I and mode-II fracture toughness of the laminates were obtained in all cases studied in [14,16], different toughening mechanisms were observed between the non-meltable PET and PPS veils and the melted PA veils. In particular, extensive thermoplastic fibre bridging was the main toughening mechanism of the non-melted PET and PPS veils, and adding the meltable PA veils mainly improved the fracture toughness of the epoxy matrix. Consequently, the different toughening mechanisms of the veils, together with the different fracture mechanisms of the laminates, significantly affected the toughening levels. The above observations in [14,16] demonstrated a possibility to take advantage of the different

* Corresponding author.
E-mail address: d.quan-1@tudelft.nl (D. Quan).

https://doi.org/10.1016/j.compstruct.2020.112699
Received 17 June 2020; Revised 5 July 2020; Accepted 13 July 2020
Available online 18 July 2020

toughening mechanisms by interlaying meltable and non-meltable veils simultaneously into the laminates, and subsequently to further enhance the interlaminar fracture toughness. Accordingly, this work presents an experimental assessment of the toughening performance of hybrid meltable/non-meltable thermoplastic veils for aerospace-grade CF/EP laminates. In particular, non-meltable PPS veils and meltable PA veils (in respect to the laminate curing temperature) were used together as hybrid interlayers of CF/EP laminates, in an effort to further improve the fracture toughness of the interleaved laminates by exploiting the different toughening mechanisms. The hybrid thermoplastic veils were used to interlay two types of aerospace-grade CF/EP laminates produced from UD prepregs and RTM of NCFs. These two laminate systems were selected as they exhibited significantly different fracture properties and mechanisms, which subsequently affected the toughening levels and mechanisms of the thermoplastic veils [14,16]. The Mode-I and Mode-II fracture behaviour and corresponding fracture mechanisms of the hybrid interleaved laminates were investigated. The results demonstrated promising effects of the hybrid veils for interlayer toughening of CF/EP laminates.

2. Experimental

Thermoplastic PPS veils with an areal density of 5 and 10 g/m^2 and PA veils with an areal density of 10 g/m^2 were supplied by Technical Fibre Products Ltd., UK. The average diameters of the PPS and PA fibres were measured to be 9.5 ± 1.1 μm and 11.7 ± 1.5 μm, respectively [14]. The melting temperatures of the PPS and the PA veils, both being semicrystalline, were determined to be 290 °C and 180 °C, respectively [14]. The UD laminates were manufactured using a prepreg method based on 26 plies of carbon fibre prepregs (HYE-1034E from Cytec, UK). The NCF laminates were produced using a vacuum-assisted RTM process from 8 plies of $[90, 0]4_s$ NCFs (biaxial Toray T700Sc 50C from Saertex GmbH, Germany) and an epoxy resin infusion system of CYCOM 890RTM from Cytec, UK. Both of the UD and NCF laminates were cured at 180 °C under a pressure of 0.5 MPa for 90 mins. It should be noted that the hybrid interlayer consisting of one layer of PPS veil and one layer of PA veil was placed at the mid-plane of the laminate during the layup process. Detailed information on the materials and the laminate manufacturing process can be found in [14]. As observed in the previous study [14,16], the PA veils melted and the PPS veils remained intact during the laminate curing process. In this work, the thermoplastic veils were referred to as the polymer type followed by the areal density of the veils. For example, PPS5 represents the PPS veils with an areal density of 5 g/m^2, and PPS5PA10 means the hybrid veils consisting of one layer of PPS5 veils and one layer of PA10 veils. Consequently, UD/PPS5PA10 represents the UD laminate interleaved by one layer of the hybrid PPS5PA10 veils.

The mode-I and mode-II fracture response of the laminates upon interlaying hybrid veils was investigated using a double cantilever beam (DCB) test [23] and an end-loaded split (ELS) test [24], respectively. A precrack with a length of 5 mm from the crack starter was generated by loading the samples under an opening mode for both of the DCB and the ELS specimens. A constant displacement rate of 2 mm/min and 1 mm/min was used for the DCB tests and the ELS tests, respectively. At least three replicate tests were conducted for each set. To analyse the fracture mechanisms of the interleaved laminates, the fracture surfaces of the specimens were imaged using an optical microscope (ZEISS Discovery V8) and a scanning electron microscope (SEM, JOEL JSM-7500F).

3. Results

3.1. Morphology of the veils in the CF/EP laminates

Figure 1 shows side-view micrographs of the interlayers within the UD and NCF laminates. The red arrows indicate the PPS fibres and the yellow arrows indicate the PA fibres. It was found that two distinct regions containing thermoplastic fibres were observed at the mid-plane of the hybrid interleaved UD laminates, i.e. PA veils on the top and PPS veils at the bottom. It was proved that the PPS fibre remained intact and the PA veils melted at the laminate curing temperature [14], and hence the PA fibres melted and then 'phase-separated' to their original fibrous shape in the hybrid interleaved UD laminates. This explained why the PA fibres and the PPS fibres exhibited different colours in Fig. 1. Only PPS fibres were observed in the interlayer regions of the hybrid interleaved NCF laminates, and the PA veils dissolved in the epoxy matrix during the curing process. Accordingly, the hybrid interlayers in the NCF laminates had a smaller thickness than their counterparts in the UD laminates, as shown in Table 1. These observations agreed well with our previous study [14], where the thicknesses of the interlayers within the laminates interleaved by solely PPS or PA veils were measured. In that work [14], it was observed that the PPS interlayers within the UD and the NCF laminates had the same thickness, and the PA interlayers within the NCF laminates possessed a much smaller thickness than their counterparts within the UD laminates. These phenomena were caused by the different fabrication processes of the laminates, i.e. prepreg for the UD laminates and RTM for the NCF laminates. Prior to the laminate curing, the epoxy resin within the UD prepreg was partially cured (at a B-stage) to provide the epoxy with film-like properties for easy handling and storage of the prepreg [25]. However, applying a B-staging process to the epoxy resin reduced its flowability and decreased the quantity of reactive groups in the resin, that negatively affected the compatibility between the thermoplastic veils and the epoxy matrix of the UD laminates. In contrast, the epoxy resin for the RTM of the NCF laminates was at a monomer state possessing high flowability and low viscosity for easy processing. Accordingly, the epoxy monomers thoroughly infused and well interacted with the hybrid PPS/PA veils during the RTM process of the NCF laminates, and resulted in good veil/epoxy compatibility. The different laminate processing methods had no effects on the thickness of the PPS veils within the UD and NCF laminates, as the PPS veils remained intact during the laminate curing process. Nevertheless, it could significantly affect the forms and thicknesses of the meltable PA veils, as shown in Fig. 1. This significantly affected the toughening performance and fracture mechanisms of the hybrid veils, as will be shown in Sections 3.2 and 3.3. As expected, the average thickness of the hybrid interlayers increased as the areal density of the PPS veils increased from 5 g/m^2 to 10 g/m^2, i.e. from 85.7 μm to 122.5 μm for the interleaved UD laminates and from 49.9 μm to 70.0 μm for the interleaved NCF laminates, see Table 1.

3.2. Mode-I fracture behaviour

Mode-I *R*-curves from the DCB tests of the laminates interleaved without and with hybrid PPS/PA veils are presented in Fig. 2. Table 2 presents the mode-I crack initiation energies (G_{IC}^{ini}) and mode-I crack propagation energies (G_{IC}^{prop}) of each specimen and the corresponding average values. In Table 2, the individual specimens for each laminate system were referred to as S1, S2 and S3, respectively. It was observed that interlaying hybrid PPS/PA veils into the UD and NCF laminates significantly improved their mode-I fracture performance in all cases. Essentially 'flat' *R*-curves were obtained for both of the UD/reference and the UD/PPS5PA10 laminates, while a 'rising' trend at the initial section of the *R*-curves was observed for the UD/PPS10PA10 laminate, indicating the presence of fibre bridging during the fracture process. Overall, G_{IC}^{ini} and G_{IC}^{prop} increased from 181 J/m^2 and 171 J/m^2 of the UD/reference laminate to 371 J/m^2 (by 105%) and 359 J/m^2 (by 110%) of the UD/PPS5PA10 laminate, respectively and further to 412 J/m^2 (by 127%) and 461 J/m^2 (by 169%) of the UD/PPS10PA10 laminate, respectively (see Table 2). For the NCF laminates, the overall

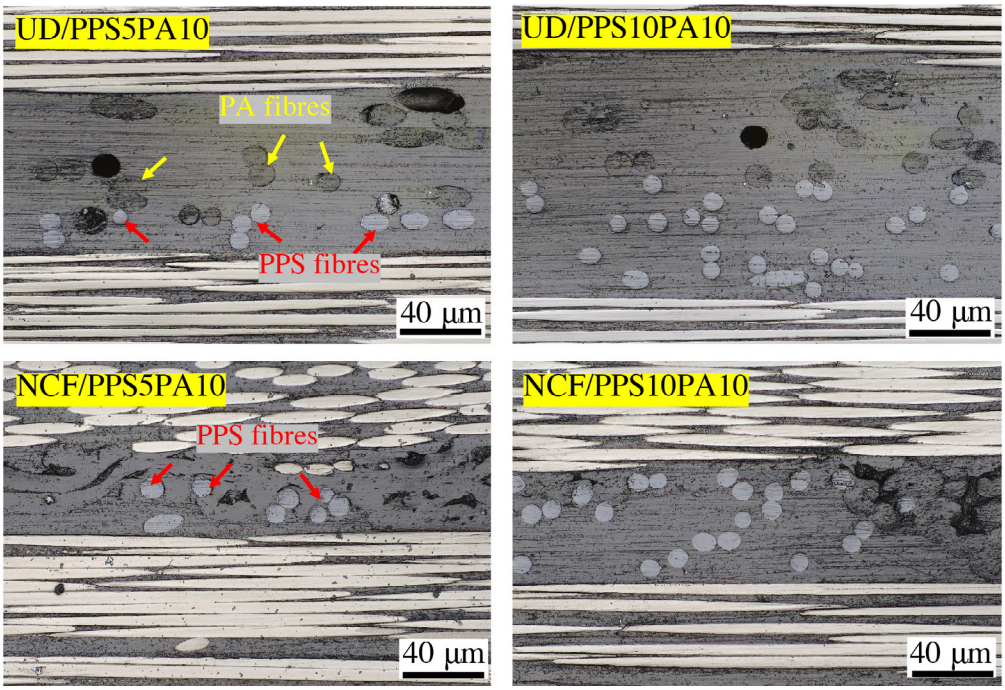

Fig. 1. Representative microscopy images of the interlayers within the interleaved laminates (side-view). The red arrows indicate the PPS fibres and the yellow arrows indicate the PA fibres.

Table 1
Average thicknesses of the hybrid interlayers in the cured laminates.

Item	UD/PPS5PA10	UD/PPS10PA10	NCF/PPS5PA10	NCF/PPS10PA10
Thickness	85.7 ± 3.3 μm	122.5 ± 6.6 μm	49.9 ± 5.2 μm	70.7 ± 2.2 μm

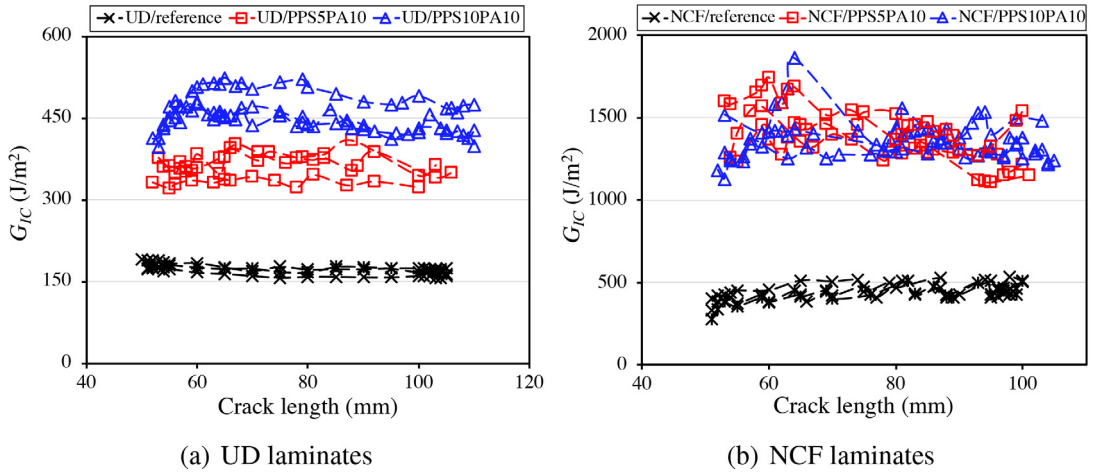

Fig. 2. Mode-I *R*-curves of the UD and NCF laminates interleaved without and with hybrid PPS/PA veils.

trend of the *R*-curves was reasonably 'flat' for the NCF laminates interleaved by hybrid PPS/PA veils. When compared to the UD laminates, more prominent improvements in the mode-I fracture energies of the NCF laminates were observed, i.e. G_{IC}^{ini} and G_{IC}^{prop} increased from 369 J/m^2 and 463 J/m^2 of the NCF/reference laminate to 1374 J/m^2 and 1366 J/m^2 of the UD/PPS5PA10 laminate, respectively. This corresponded to an increase of 273% and 195%, respectively. No further improvements in G_{IC}^{ini} and G_{IC}^{prop} were observed as the areal density of the PPS veils increased from 5 g/m^2 to 10 g/m^2.

Fig. 3 presents representative photographs and optical microscopy images of the mode-I fracture surfaces and cross-sections of the interleaved laminates, taking from the corresponding S1 DCB specimens. The yellow arrows indicate delaminated bundles of carbon fibres, and the red dashed boxes indicate the interlayers. It was observed that the crack propagated cohesively inside the veil/epoxy layer for the hybrid modified UD laminates, leaving both sides of the fracture surfaces covered with numerous thermoplastic fibres. An alternation of cohesive failure inside the interlayer and significant carbon fibre

Table 2
Mode-I fracture energies of each specimen (indicated by S1–S3) and the corresponding average values from the DCB tests of the laminates. Values in brackets indicate percentage increases of the values over those of reference specimens.

Material	G_{IC}^{ini} (J/m^2)				G_{IC}^{prop} (J/m^2)			
	S1	S2	S3	Average	S1	S2	S3	Average
UD/reference	191	175	177	181 ± 9	178	173	163	171 ± 8
UD/PPS5PA10	379	331	402	371 ± 36 (105%)	379	331	368	359 ± 25 (110%)
UD/PPS10PA10	412	392	431	412 ± 20 (127%)	494	444	445	461 ± 29 (169%)
NCF/reference	370	340	396	369 ± 28	455	452	480	463 ± 15
NCF/PPS5PA10	1310	1352	1460	1374 ± 77 (273%)	1287	1503	1309	1366 ± 119 (195%)
NCF/PPS10PA10	1324	1176	1509	1337 ± 166 (263%)	1402	1267	1400	1357 ± 77 (193%)

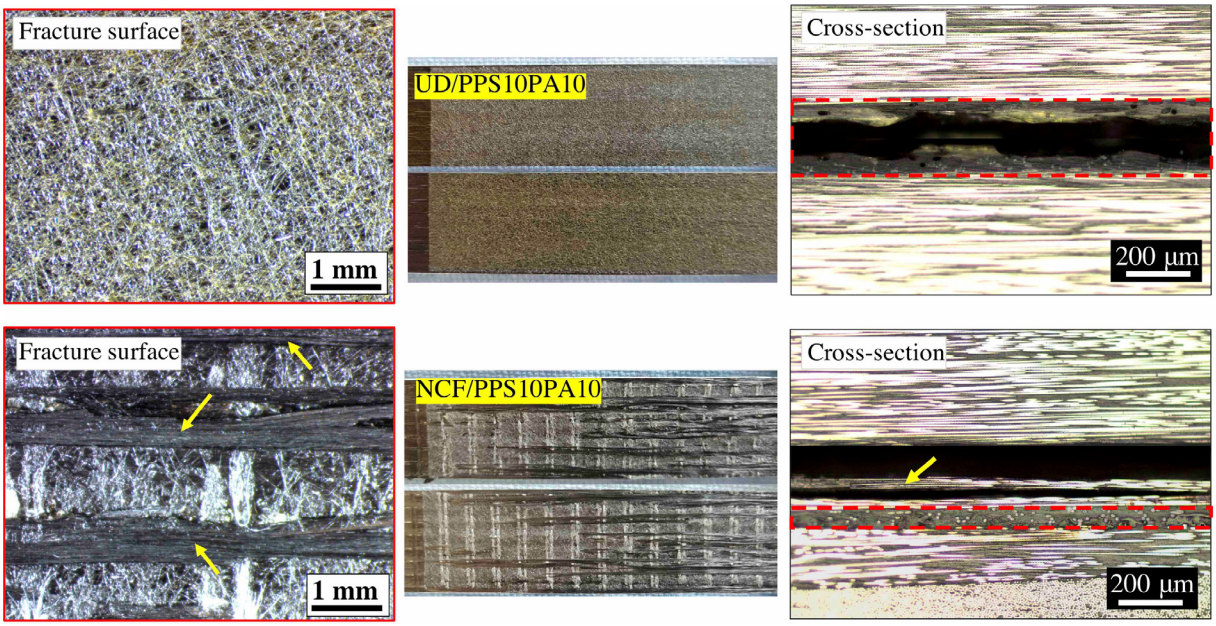

Fig. 3. Representative photographs (in the middle) and corresponding optical microscopy images of the fracture surfaces (on the left) and cross-sections (on the right) of the DCB specimens, taking from the corresponding S1 specimens. The yellow arrows indicate delaminated bundles of carbon fibres. The red dashed boxes indicate the interlayers.

delamination took place for the hybrid interleaved NCF laminates. Representative SEM images for showing the state of the thermoplastic veils on the fracture surfaces are shown in Figure 4. It was observed that a large number of relatively long thermoplastic fibres appeared on the fracture surfaces of both of the UD/PPA10PA10 and NCF/PPS10PA10 laminates, see Fig. 4(a) and (d). These were the pulled-out PPS fibres, who possessed very smooth surfaces and exhibited no visible damage to the fibres themselves as a result of a poor PPS/epoxy adhesion, as shown in Fig. 4(b) and (e). As observed in Section 3.1, the meltable PA fibres remained in a fibrous form on the fracture surfaces of the hybrid modified UD laminates, while they completely melted in the hybrid modified NCF laminates, see Fig. 4(c) and (f). Accordingly, different toughening mechanisms of the PA veils were observed in different cases. For the interleaved UD laminates, the PA fibres broke into small pieces that were still well-attached to the epoxy matrix, see Fig. 4 (c). This indicates a relatively good adhesion between the meltable PA fibres and the epoxy matrix, resulting in significant plastic deformation and following breakage of the PA fibres during the fracture process. For the interleaved NCF laminates, the PA veils mainly toughened the epoxy matrix and resulted in obvious plastic deformation of the epoxy/PA mixture for the interleaved NCF laminates (as shown in Fig. 4 (f)). In summary, the toughening mechanisms of the hybrid veils for the UD laminates were pulling-out and bridging of the PPS fibres and significant damage of the PA fibres. For the NCF laminates, fibre pulling-out and bridging were also determined to be the main toughening mechanisms of the PPS veils, while the PA veils toughened the epoxy matrix and resulted in significant plastic deformation during the mode-I fracture process. These mechanisms, together with additional carbon fibre delamination and breakage (see Fig. 3), resulted in the significant increases in G_{IC} of the NCF laminates upon interlaying the hybrid veils, as shown in Table 2.

It remained to be answered why the areal density of the PPS veils exhibited different influences on the toughening performance of the hybrid veils for the UD and NCF laminates, as observed in Fig. 2. Typical SEM images of the mode-I fracture surfaces of the laminates interleaved with PPS5PA10 veils are shown in Fig. 5. It was observed that only a number of pulled-out PPS fibres existed on the mode-I fracture surface of the UD/PPS5PA10 laminate, with the remaining PPS fibres well-embedded in the epoxy matrix. This indicates a low level of PPS fibre bridging during the fracture process. However, as the areal density of the PPS veils increased from 5 g/m^2 to 10 g/m^2, many pulled-out PPS fibres in a long and continuous form were observed on the fracture process of the UD/PPS10PA10 laminate, as shown in Fig. 4 (a). This resulted from significant PPS fibre bridging during the fracture process, and led to the 'rising' trend of the mode-I *R*-curves and further increases in the mode-I fracture energies of the UD/PPS10PA10 laminate, see Fig. 2. In contrast, a comparison between Figs. 4(d) and 5(b) showed that the fracture surfaces of the NCF/

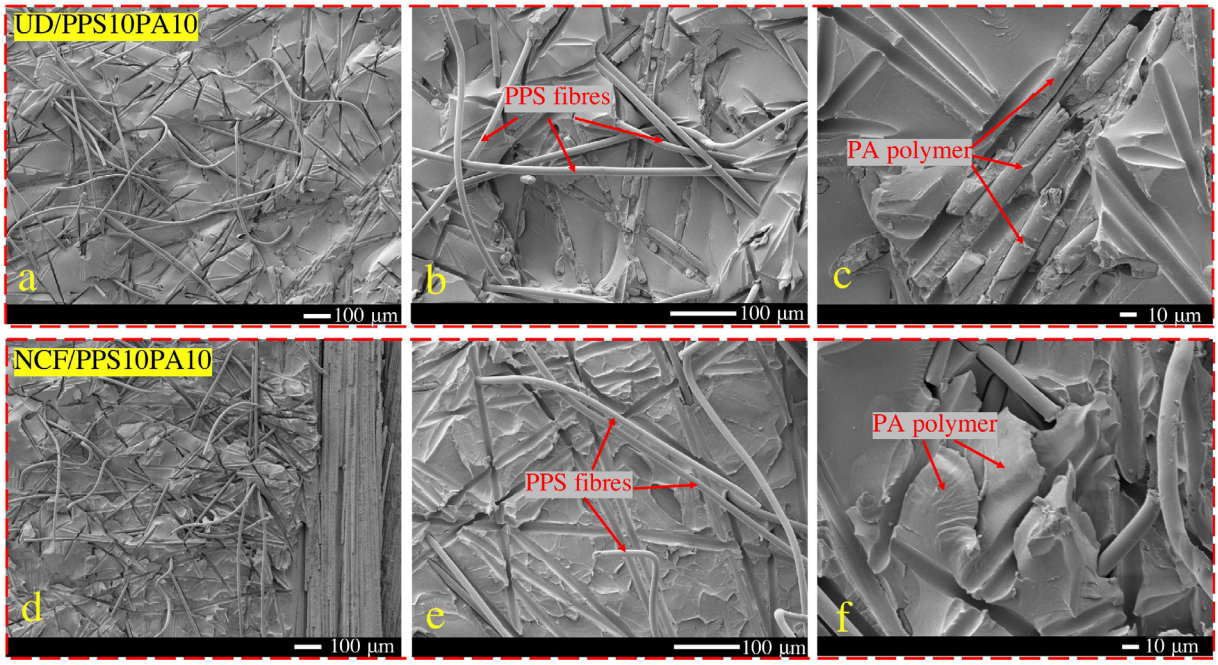

Fig. 4. Representative SEM images of the mode-I fracture surfaces of the hybrid interleaved UD and NCF laminates. (a)–(c) are the images for the UD/PPS10PA10 laminate, and (d)–(f) are the images for the NCF/PPS10PA10 laminate.

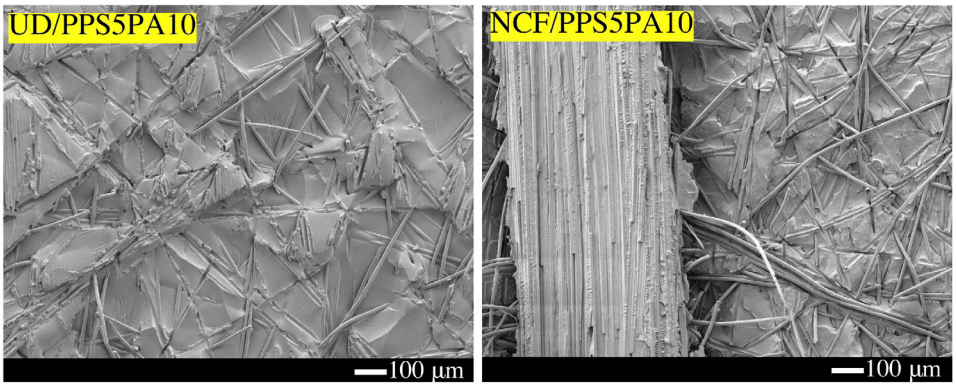

Fig. 5. Representative SEM images of the mode-I fracture surfaces of the laminates interleaved with PPS5PA10 veils.

PPS5PA10 and the NCF/PPS10PA10 laminates appeared essentially the same. Accordingly, the areal density of the PPS veils had negligible effects on the mode-I fracture energies of the hybrid interleaved NCF laminates, as shown in Fig. 2.

3.3. Mode-II fracture behaviour

Fig. 6 shows the mode-II *R*-curves from the ELS tests of the laminates interleaved without and with hybrid PPS/PA veils. During the ELS test, the specimens of the UD laminates interleaved with hybrid veils failed dynamically once the crack propagation initiated, resulting in only one point on the corresponding *R*-curves in Fig. 6(a). Similarly, the ELS specimens of the NCF/reference laminate failed dynamically after the crack propagated a few millimetres, and hence only a number of points exist on their *R*-curves in Fig. 6(b). It is clear that the addition of hybrid PPS/PA veils improved the mode-II fracture performance of the UD and NCF laminates in all cases. Moreover, it also alternated the crack propagation from a stable manner to a dynamic manner for the UD laminates and from a dynamic manner to a stable manner for the NCF laminates. The mode-II crack initiation energies (G_{IIC}^{ini}) and mode-II crack propagation energies (G_{IIC}^{prop}) of each specimen and the corresponding average values are presented in Table 3. It should be noted that no plateau stage was obtained on the *R*-curves of the interleaved UD laminates and the NCF reference laminate due to a dynamic failure. In this case, G_{IIC}^{prop} was taken as the fracture energy before the dynamic failure of the specimen, i.e. the last point on the *R*-curve. It was observed that interlaying PPS/PA veils into the UD laminates significantly increased both of G_{IIC}^{ini} and G_{IIC}^{prop} by about 130% in all cases. For the NCF laminates, G_{IIC}^{ini} and G_{IIC}^{prop} increased from 1185 J/m^2 and 2549 J/m^2 to 3378 J/m^2 (by 185%) and 4148 J/m^2 (by 63%), respectively upon interleaving the PPS5PA10 veils. No statistical differences in G_{IIC}^{ini} and G_{IIC}^{prop} were observed as the areal density of the PPS veils increased from 5 g/m^2 to 10 g/m^2 for both of the UD and the NCF laminates.

Fig. 7 presents representative photographs and microscopy images of the fracture surfaces and cross-sections of the ELS specimens for the

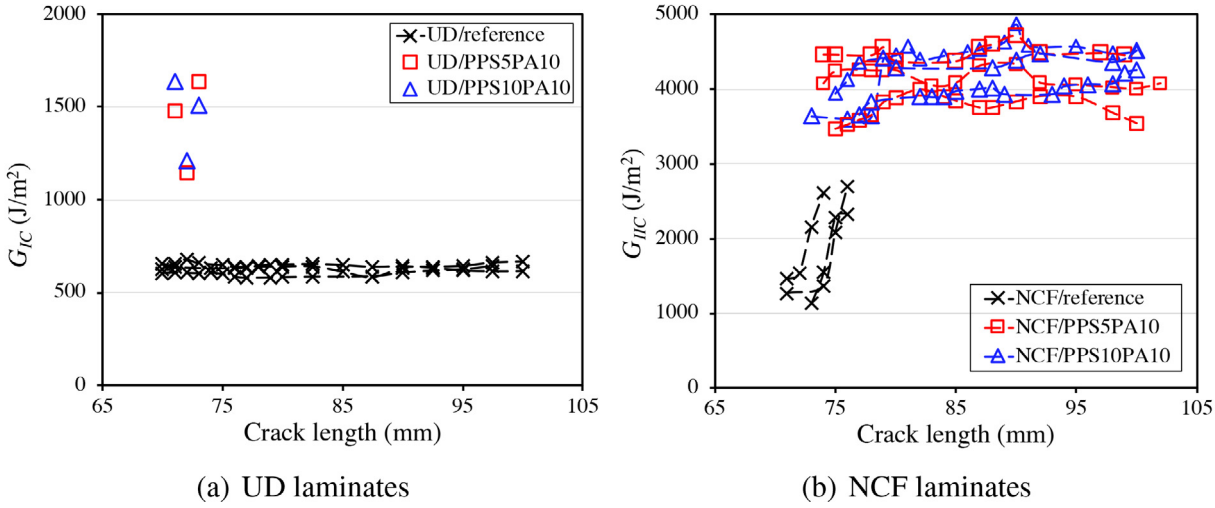

Fig. 6. Mode-II *R*-curves of the UD and NCF laminates interleaved with hybrid PPS/PA veils.

Table 3
Mode-II fracture energies of each specimen (indicated by S1–S3) and the corresponding average values from the ELS tests of the laminates. Values in brackets indicate percentage increases of the values over those of reference specimens.

Material	G_{IIC}^{ini} (J/m^2)				G_{IIC}^{prop} (J/m^2)			
	S1	S2	S3	Average	S1	S2	S3	Average
UD/reference	657	629	605	630 ± 26	634	643	602	627 ± 22
UD/PPS5PA10	1638	1147	1482	1422 ± 251 (126%)	1638	1147	1482	1422 ± 251 (127%)
UD/PPS10PA10	1211	1635	1509	1452 ± 218 (130%)	1211	1635	1509	1452 ± 218 (132%)
NCF/reference	1261	1053	1242	1185 ± 115	2702	2333	2613	2549 ± 192
NCF/PPS5PA10	3343	3325	3467	3378 ± 77 (185%)	4157	3786	4503	4148 ± 358 (63%)
NCF/PPS10PA10	3320	4010	3558	3629 ± 350 (206%)	4096	4597	4436	4376 ± 256 (72%)

interleaved UD laminates, taking from the corresponding S1 specimen. It was observed that the crack propagation migrated from within the veil/epoxy layer (resulted from the pre-cracking process under an opening load) to the interface between the carbon fibres and the veil/epoxy layer, and then dynamically failed the entire ELS specimens. Consequently, the entire veil/epoxy layer (with all the thermo-

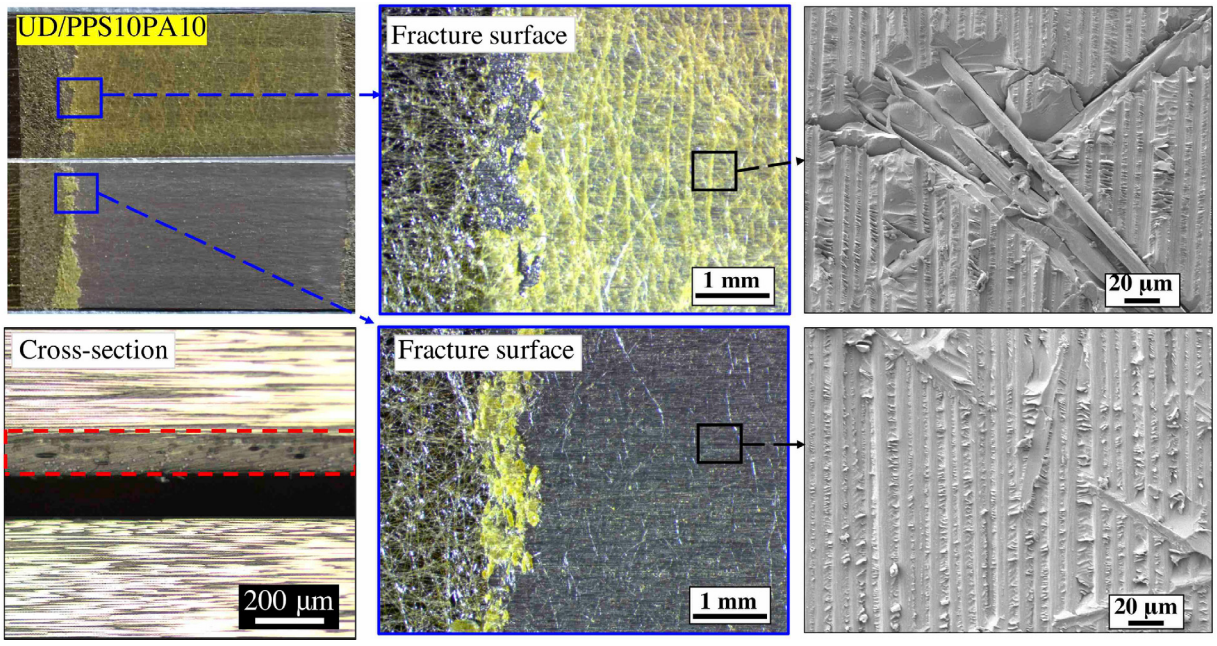

Fig. 7. Representative photographs and microscopy images of the fracture surfaces and cross-section of an ELS specimen of the hybrid interleaved UD laminates. The red dashed box in the cross-section image indicates the interlayer.

plastic fibres embedded within it) was left on the upper fracture surface, with the lower fracture surface showing bare carbon fibres. In this case, the areal density of the PPS veils tended to have no effects on the mode-II fracture mechanisms and the fracture energies of the interleaved UD laminates, as shown in Table 3. Representative photographs and microscopy images of the fracture surfaces and cross-sections of the ELS specimens for the hybrid modified NCF laminates are shown in Figure 8. An alternation of cohesive failure inside the veil/epoxy layer and carbon fibre delamination was observed for the hybrid interleaved NCF laminates. The presence of a large number of leaf-like features (indicated by the red arrows in Fig. 8) indicates extensive plastic deformation of the PA toughened epoxy matrix during the fracture process. Additionally, significant damage to the pulled-out PPS fibres, i.e. fibre split, plastic deformation and breakage, took place during the fracture process of the interleaved NCF laminates, as indicated by the blue arrows in Fig. 8. It should be noted that, our previous work demonstrated that the PPS fibres on the fracture surfaces of the NCF laminates interleaved with solely PPS veils remained intact [16], as shown in Fig. 9. This demonstrated that the presence of melted PA polymers in the epoxy matrix improved the adhesion between the PPS fibres and the matrix, that resulted in significant damage to the PPS fibres during the fracture process, and further improved their toughening performance [26]. Overall, plastic deformation of the PA toughened epoxy, severe damage to the PPS fibres and significant carbon fibre delamination all contributed to the significant increases in the mode-II fracture energy of the NCF laminates upon interlaying the hybrid veils.

3.4. Discussion

The mode-I and mode-II fracture energies of the UD and NCF laminates interleaved with PPS veils and PA veils on their own [14,16] and in combination are summarised in Fig. 10. Obviously, significant increases in the fracture toughness of the UD and NCF laminates were achieved upon interleaving thermoplastic veils in all cases. For the UD laminates, the toughening performance of hybrid PPS/PA veils was superior for the mode-I fracture behaviour, i.e. adding hybrid PPS/PA veils increased the mode-I fracture energies to a higher level that was not attained by interleaving the PPS veils or the PA veils alone, see Fig. 10(a). This was achieved by simultaneously taking advantage of the fiber bridging mechanism of the non-meltable PPS veils and the significant fibres damage of the meltable PA fibres, as observed in Section 3.2. Regarding mode-II fracture behaviour, the PA veils alone worked better for toughening the UD laminate than all the other interlayer systems. A hybridisation of the PA veils with the PPS veils failed to further improve the mode-II fracture energies of the interleaved UD laminate, and even caused significant adverse effects. This was due to the alteration of the crack propagation characteristic from a cohesive failure inside the veils/epoxy layer to an interfacial failure between the interlayers and the carbon fibres, as shown in Section 3.3. For this reason, the toughening mechanisms of both of the PPS veils and the PA veils were not sufficiently utilised. For the NCF laminates, the toughening performance of hybrid PPS/PA veils was outstanding for both of the mode-I and mode-II fracture energies, as shown in Fig. 10(b)

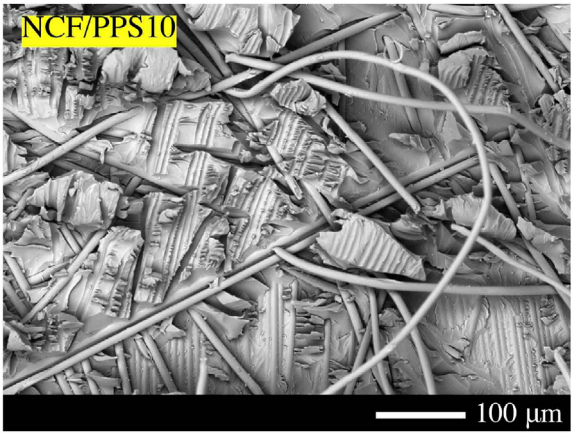

Fig. 9. A representative SEM image of the mode-II fracture surfaces of the NCF laminates interleaved with solely PPS veils [16].

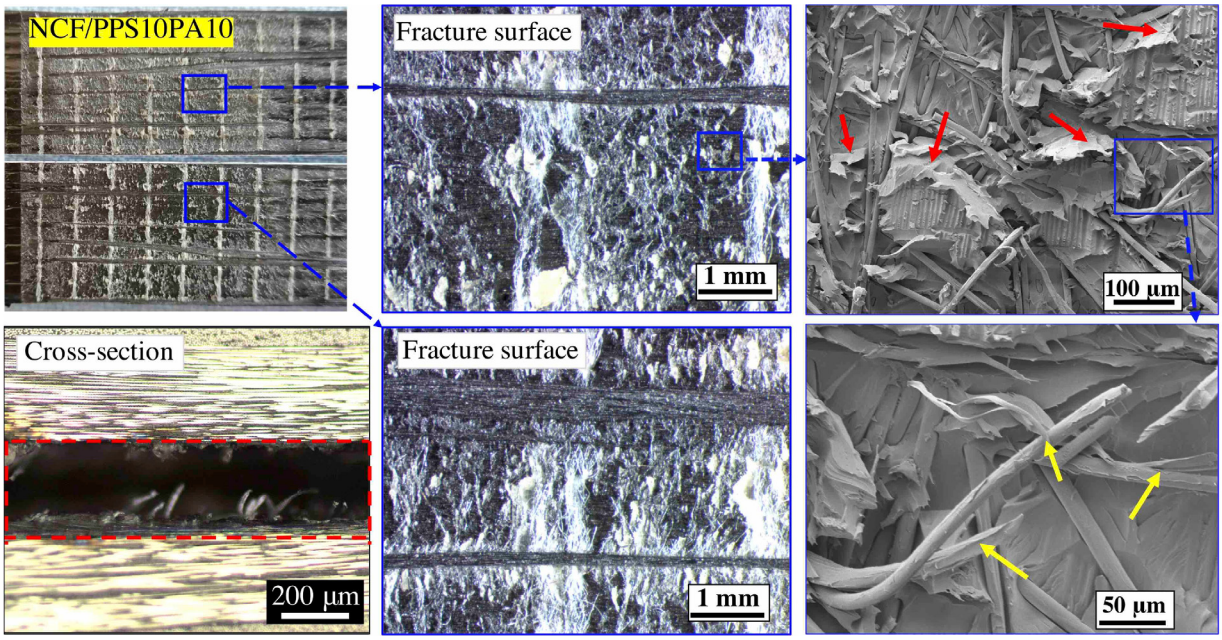

Fig. 8. Representative photographs and microscopy images of the fracture surfaces and cross-section of an ELS specimen of the hybrid interleaved NCF laminates. The red arrows indicate the PA/epoxy mixture and the yellow arrows indicate the damaged PPS fibres. The red dashed box in the cross-section image indicates the interlayer.

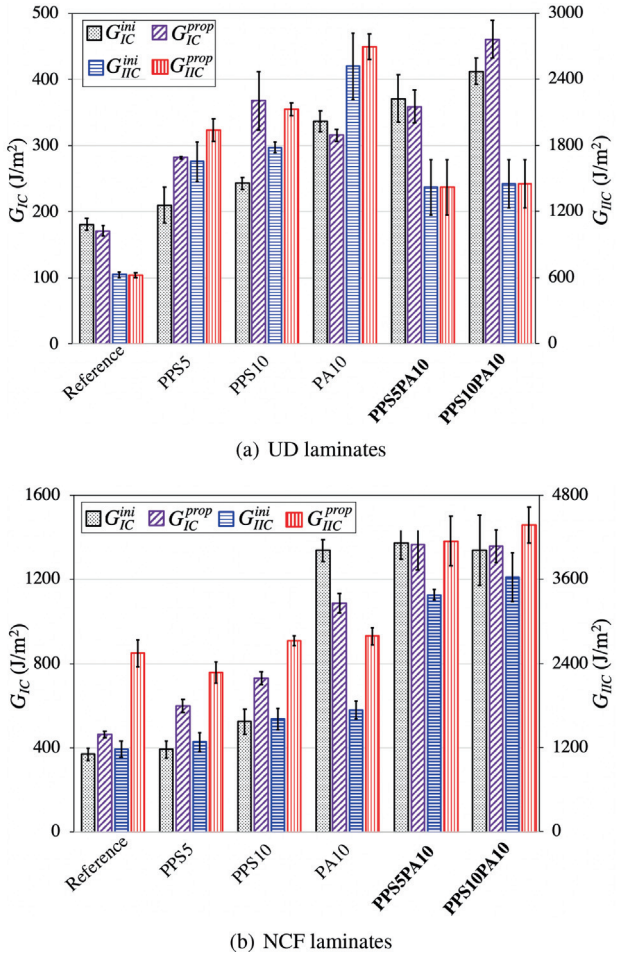

Fig. 10. Comparison of the fracture energies of the UD and NCF laminates interleaved with different thermoplastic veils.

by exploiting different toughening mechanisms of the hybrid veils. In particular, fibre pulling-out and bridging of the PPS veils and epoxy toughening and plastic deformation of the PA veils were determined to be the main toughening mechanisms of the hybrid veils for the mode-I fracture behaviour of the NCF laminates, as observed in Sections 3.2. Apart from these mechanisms, additional PPS fibre breakage also took place during the mode-II fracture process of the NCF laminates, see Sections 3.2. Overall, interlaying hybrid PPS/PA veils proved a very promising strategy for enhancing the mode-I fracture performance of the UD laminate and the mode-I and mode-II fracture performance of the NCF laminates. Considering the already outstanding toughening efficiency of the PPS and PA veils (on their own) when compared to the other most effective state-of-the-art interlayer materials [1,16,27], the hybrid PPS/PA veils were superior for interlay toughening of CF/EP laminates. Emphasis should be given to two important observations from this work. Firstly, the adhesion between the thermoplastic veils and the epoxy matrix significantly affected the toughening performance of the thermoplastic veils. In particular, the veil/epoxy adhesion was largely affected by the manufacturing methods of the laminates in this work, i.e. a partially cured state of the epoxy resin in the UD prepreg resulted in relatively poor veil/epoxy compatibility while the epoxy monomers for the RTM of the NCF laminates effectively interacted with the veils during the laminate curing process. Secondly, the presence of the meltable PA veils obviously improved the adhesion between the PPS veils and the epoxy matrix coupled with melted PA polymers within the interleaved NCF laminates. This further enhanced the toughening performance of the PPS veils, and subsequently resulted in the outstanding toughening effects of the hybrid PPS/PA veils for the NCF laminates.

4. Conclusions

Non-meltable PPS veils and meltable PA veils were hybridised as interlayer materials of two types of aerospace-grade CF/EP laminates produced from UD prepregs and RTM of NCFs, with an attempt to improve their interlaminar fracture toughness. In general, the addition of the hybrid veils significantly improved the fracture toughness of the laminates in all cases. For the UD laminates, interlaying the hybrid veils resulted in significant improvements of the mode-I fracture energies those could not be achieved by solely interlaying the meltable or non-meltable veils on their own. This was achieved by taking advantage of the different toughening mechanisms of the hybrid veils, i.e. fibre pulling-out and bridging of the PPS veils and severe fibre damage of the PA veils. Unfortunately, the mode-II crack propagation in the interleaved UD laminates took place at the interface between the veil/epoxy layer and the carbon fibres. In this case, the toughening mechanisms of the hybrid veils were not sufficiently utilised, and hence the toughening levels of the hybrid veils were lower than their individual components. Encouragingly, the hybrid veils exhibited outstanding toughening performance for both of the mode-I and mode-II fracture behaviour of the NCF laminates. This was achieved by exploiting the different toughening mechanisms of the non-meltable and meltable veils, i.e. extensive PPS fibre pulling-out, bridging and breakage of the PPS veils, and epoxy toughening and associated carbon fibre delamination of the PA veils. This work demonstrated that interlaying hybrid non-meltable/meltable veils into CF/EP laminates is a promising strategy to further enhance the interlaminar fracture toughness of the laminates, and the compatibility between the epoxy matrix and the veils is a critical factor affecting the toughening levels and mechanisms.

Data availability

The raw/processed data required to reproduce these findings cannot be shared at this time due to legal or ethical reasons.

Declaration of Competing Interest

The authors declare that they have no known competing financial interests or personal relationships that could have appeared to influence the work reported in this paper.

Acknowledgements

This work is funded by the European Union's Horizon 2020 research and innovation programme (under the Marie Skłodowska-Curie grant agreement No. 842467) and Irish Composites Centre. We would like to thank Bombardier Aerospace (UK) and Technical Fibre Products (UK) for supplying the carbon fibre fabrics and thermoplastic veils.

References

[1] Quan D, Mischo C, Binsfeld L, Ivankovic A, Murphy N. Fracture behaviour of carbon fibre/epoxy composites interleaved by MWCNT- and graphene nanoplatelet-doped thermoplastic veils. Compos Struct 2020;235. https://doi.org/10.1016/j.compstruct.2019.111767. 111767.

[2] Shin YC, Lee WI, Kim HS. Mode II interlaminar fracture toughness of carbon nanotubes/epoxy film-interleaved carbon fiber composites. Compos Struct 2020;236. https://doi.org/10.1016/j.compstruct.2019.111808. 111808.

[3] Wang J, Ma C, Chen G, Dai P. Interlaminar fracture toughness and conductivity of carbon fiber/epoxy resin composite laminate modified by carbon black-loaded polypropylene non-woven fabric interleaves. Compos Struct 2020;234. https://doi.org/10.1016/j.compstruct.2019.111649. 111649.

[4] Liu B, Gao N, Cao S, Ye F, Liu Y, Zhang Y, Cheng L, Kikuchi M. Interlaminar toughening of unidirectional CFRP with multilayers graphene and MWCNTs for Mode II fracture. Compos Struct 2020;236. https://doi.org/10.1016/j.compstruct.2020.111888. 111888.
[5] Yao J, Niu K, Niu Y, Zhang T. Toughening efficiency and mechanism of carbon fibre epoxy matrix composites by PEK-C. Compos Struct 2019;229. https://doi.org/10.1016/j.compstruct.2019.111431. 111431.
[6] Yao J, Zhang T, Niu Y. Effect of curing time on phase morphology and fracture toughness of pek-c film interleaved carbon fibre/epoxy composite laminates. Compos Struct 2020;248. https://doi.org/10.1016/j.compstruct.2020.112550. 112550.
[7] Cugnoni J, Amacher R, Kohler S, Brunner J, Kramer E, Dransfeld C, Smith W, Scobbie K, Sorensen L, Botsis J. Towards aerospace grade thin-ply composites: effect of ply thickness, fibre, matrix and interlayer toughening on strength and damage tolerance. Compos Sci Technol 2018;168:467–77. https://doi.org/10.1016/j.compscitech.2018.08.037.
[8] Arnold M, Henne M, Bender K, Drechsler K. The influence of various kinds of PA12 interlayer on the interlaminar toughness of carbon fiber-reinforced epoxy composites. Polym Compos 2015;36(7):1249–57. https://doi.org/10.1002/pc.23029.
[9] Zhou H, Du X, Liu H-Y, Zhou H, Zhang Y, Mai Y-W. Delamination toughening of carbon fiber/epoxy laminates by hierarchical carbon nanotube-short carbon fiber interleaves. Compos Sci Technol 2017;140:46–53. https://doi.org/10.1016/j.compscitech.2016.12.018.
[10] Quan D, Flynn S, Artuso M, Murphy N, Rouge C, Ivankovic A. Interlaminar fracture toughness of CFRPs interleaved with stainless steel fibres. Compos Struct 2019;210:49–56. https://doi.org/10.1016/j.compstruct.2018.11.016.
[11] Nash N, Young T, McGrail P, Stanley W. Inclusion of a thermoplastic phase to improve impact and post-impact performances of carbon fibre reinforced thermosetting composites—a review. Mater Des 2015;85:582–97. https://doi.org/10.1016/j.matdes.2015.07.001.
[12] Beylergil B, Tanoglu M, Aktas E. Enhancement of interlaminar fracture toughness of carbon fiber/epoxy composites using polyamide-6,6 electrospun nanofibers. J Appl Polym Sci 2017;134(35):45244. https://doi.org/10.1002/app.45244.
[13] Palazzetti R, Zucchelli A, Trendafilova I. The self-reinforcing effect of Nylon 6,6 nano-fibres on CFRP laminates subjected to low velocity impact. Compos Struct 2013;106:661–71. https://doi.org/10.1016/j.compstruct.2013.07.021.
[14] Quan D, Bologna F, Scarselli G, Ivankovic A, Murphy N. Interlaminar fracture toughness of aerospace-grade carbon fibre reinforced plastics interleaved with thermoplastic veils. Compos A Appl Sci Manuf 2020;128. https://doi.org/10.1016/j.compositesa.2019.105642. 105642.
[15] Wong DW, Lin L, McGrail PT, Peijs T, Hogg PJ. Improved fracture toughness of carbon fibre/epoxy composite laminates using dissolvable thermoplastic fibres. Compos A Appl Sci Manuf 2010;41(6):759–67. https://doi.org/10.1016/j.compositesa.2010.02.008.
[16] Quan D, Bologna F, Scarselli G, Ivankovi A, Murphy N. Mode-II fracture behaviour of aerospace-grade carbon fibre/epoxy composites interleaved with thermoplastic veils. Compos Sci Technol 2020;191. https://doi.org/10.1016/j.compscitech.2020.108065. 108065.
[17] Li G, Li P, Zhang C, Yu Y, Liu H, Zhang S, Jia X, Yang X, Xue Z, Ryu S. Inhomogeneous toughening of carbon fiber/epoxy composite using electrospun polysulfone nanofibrous membranes by in situ phase separation. Compos Sci Technol 2008;68(3):987–94. https://doi.org/10.1016/j.compscitech.2007.07.010.
[18] Daelemans L, van der Heijden S, Baere ID, Rahier H, Paepegem WV, Clerck KD. Nanofibre bridging as a toughening mechanism in carbon/epoxy composite laminates interleaved with electrospun polyamide nanofibrous veils. Compos Sci Technol 2015;117:244–56. https://doi.org/10.1016/j.compscitech.2015.06.021.
[19] Beylergil B, Tanoglu M, Aktas E. Effect of polyamide-6,6 (PA 66) nonwoven veils on the mechanical performance of carbon fiber/epoxy composites. Compos Struct 2018;194:21–35. https://doi.org/10.1016/j.compstruct.2018.03.097.
[20] Molnar, LMK, Kostakova E. The effect of needleless electrospun nanofibrous interleaves on mechanical properties of carbon fabrics/epoxy laminates. eXPRESS Polym Lett 8 (1): 2014; 62–72. doi:10.3144/expresspolymlett.2014.8..
[21] Beylergil B, Tanoglu M, Aktas E. Modification of carbon fibre/epoxy composites by polyvinyl alcohol (PVA) based electrospun nanofibres. Adv Compos Lett 2016;25(3):69–76. https://doi.org/10.1177/096369351602500303.
[22] Beylergil B, Tanoglu M, Aktas E. Mode-I fracture toughness of carbon fiber/epoxy composites interleaved by aramid nonwoven veils. Steel Compos Struct 2019;31(2):113–23. https://doi.org/10.12989/scs.2019.31.2.113.
[23] BS ISO 15024:2001. Fibre-reinforced plastic composites Determination of mode I interlaminar fracture toughness, G_{IC} for unidirectionally reinforced materials; 2001..
[24] ISO 15114:2014. Fibre-reinforced plastic composites Determination of mode II fracture resistance for unidirectionally reinforced materials using the calibrated end-loaded split (C-ELS) test and an effective crack length approach; 2014..
[25] Costantino S, Waldvogel U. Composite processing: state of the art and future trends. In: Pascault J-P, Williams RJJP, editors. Epoxy polymers. John Wiley & Sons Ltd; 2010. p. 275–7.
[26] Quan D, Deegan B, Alderliesten R, Dransfeld C, Murphy N, Ivankovic A, Benedictus R. The influence of interlayer/epoxy adhesion on the mode-I and mode-II fracture response of carbon fibre/epoxy composites interleaved with thermoplastic veils. Mater Des 2020;108781. https://doi.org/10.1016/j.matdes.2020.108781.
[27] Quan D, Deegan B, Binsfeld L, Li X, Atkinson J, Ivankovic A, Murphy N. Effect of interlaying UV-irradiated PEEK fibres on the mechanical, impact and fracture response of aerospace-grade carbon fibre/epoxy composites. Compos B Eng 2020;191. https://doi.org/10.1016/j.compositesb.2020.107923. 107923.